JOURNAL OF THERMOPHYSICS AND HEAT TRANSFER
Vol. 8, No. 1, Jan.–March 1994

Mixed Convection Along an Isothermal Vertical Cylinder in Porous Media

W. B. Hooper,* T. S. Chen,† and B. F. Armaly‡
University of Missouri—Rolla, Rolla, Missouri 65401

Mixed convection adjacent to a vertical cylinder in porous media is studied. The problem is solved using the nonsimilarity solution method for the case of uniform wall temperature (UWT). In the first approach, mixed convection is studied by examining separately the buoyancy effect on forced convection and the forced flow effect on free convection. These effects are represented, respectively, by Ra_x/Pe_x and Pe_x/Ra_x. Curvature is represented by $\xi_f = (x/r_0)Pe_x^{-1/2}$ in the forced-convection-dominated regime and by $\xi_n = (x/r_0)Ra_x^{-1/2}$ in the free-convection-dominated regime. The second approach examines the entire regime of mixed convection by introducing the single parameter $\chi = [1 + (Ra_x/Pe_x)^{1/2}]^{-1}$, where $\chi = 1$ corresponds to pure forced convection and $\chi = 0$ to pure free convection. In this regime, the curvature is represented by $\xi = (x/r_0)[Pe_x^{1/2} + Ra_x^{1/2}]^{-1}$. In the analysis, the non-Darcian and thermal dispersion effects are neglected. The resulting nonsimilar systems of equations from the different approaches are solved using a finite difference method. Results are presented for temperature and velocity profiles, and local Nusselt number. Correlation equations are given for local and average Nusselt numbers in all regimes of mixed convection.

Nomenclature

f = dimensionless stream function
$h(x)$ = local heat transfer coefficient
$\bar{h}$ = average heat transfer coefficient, $(1/L)\int_0^L h\,dx$
K = permeability coefficient of the porous medium
k = thermal conductivity
L = length of the cylinder
Nu_x = local Nusselt number, hx/k
$\overline{Nu}$ = average Nusselt number, $\bar{h}L/k$
Pe_x = local Peclet number, $u_\infty x/\alpha$
q_w = local surface heat flux
Ra_x = local Rayleigh number, $g\beta|T_w - T_\infty|Kx/(\nu\alpha)$
T = temperature
T_w = wall temperature
T_∞ = freestream temperature
u, v = velocity components in the x and r directions
u_∞ = freestream velocity
x, r = axial and radial coordinates
α = effective thermal diffusivity of saturated porous medium
β = volumetric coefficient of thermal expansion
η = pseudosimilarity variable
θ = dimensionless temperature
μ = dynamic viscosity
ν = kinematic viscosity
ξ = curvature parameter
ρ = fluid density
τ_w = local wall shear stress
ψ = stream function
χ = mixed convection parameter, Eq. (30)
Ω = buoyancy parameter

Subscripts
f = forced-convection regime
n = natural- (or free-) convection regime
m = mixed-convection regime
∞ = freestream condition

Received July 29, 1992; revision received Feb. 24, 1993; accepted for publication Feb. 24, 1993.

*Graduate Research Assistant, Department of Mechanical and Aerospace Engineering and Engineering Mechanics.
†Curators' Professor, Department of Mechanical and Aerospace Engineering and Engineering Mechanics. Associate Fellow AIAA.
‡Chairman and Professor, Department of Mechanical and Aerospace Engineering and Engineering Mechanics. Member AIAA.

Introduction

THERE have been a great deal of studies dealing with convective heat transfer along vertical impermeable surfaces in a porous medium.[1-11] Many studies have been conducted on natural or mixed convection under Darcy's law,[1,2,7-12] which has been found to be valid under low freestream velocity and small porosity.[5] Additionally, most of the analyses in the past have been confined to similar boundary layers.[1,5,6] However, most practical problems involving mixed convection in boundary-layer flows are nonsimilar. Solutions of nonsimilar boundary-layer flow problems have traditionally involved the similarity, local similarity, and local nonsimilarity methods. The local similarity solution has been found to be in error by 10–15% when compared to the local nonsimilarity solution.[12] Hsieh et al.[5,6] and Aldoss et al.[10-12] have studied the problem of nonsimilar mixed-convection flow along vertical and horizontal plates in porous media. Some studies involving curved surfaces have also been conducted for natural-convection along a vertical cylinder[2] and mixed convection over horizontal cylinders and spheres.[12] Mixed convection along vertical cylinders is important in situations encountered in the areas of geothermal power generation and petroleum drilling when freestream velocity may be varied from a very small to a very large value. This variation in freestream velocity along with induced buoyancy force due to changes in fluid density (as the result of temperature variation) gives rise to situations that are encountered in the regime of mixed convection.

In this article, mixed convection from an isothermal vertical cylinder embedded in a porous medium is analyzed based on the Darcy model (without the inertia and no-slip boundary effects), along with the assumption of uniform porosity and the neglect of thermal dispersion effects. The viscous shearing stress term in the momentum equation can be neglected if the particle diameter is small in comparison with the cylinder diameter. The thermal dispersion effect can be significant when the inertia effects are prevalent.[13] However, the thermal dispersion term in the energy equation can be neglected when the inertia effect is small, such as in the free-convection-dominated mixed-convection regime. For forced-convection-dominated mixed-convection regime, thermal dispersion effects

should be included. However, since there is still a great deal of controversy on the thermal dispersion theory,[14] this effect is not taken into consideration in the forced-convection-dominated mixed-convection regime of the present problem. Because of the surface curvature and the buoyancy effect, the temperature and flowfields are nonsimilar. The analysis is carried out for forced-convection-dominated mixed-convection regime, free-convection-dominated mixed-convection regime, and mixed convection for the entire regime (from pure forced convection to pure free convection). The governing conservation equations are first transformed into a dimensionless form by employing transformation variables that are appropriate for each mixed-convection regime. The parameter Ra_x/Pe_x is found to characterize the effect of buoyancy on forced convection, whereas its inverse, Pe_x/Ra_x, is found to characterize the effect of forced flow on free convection. The corresponding nonsimilarity parameters are $\xi_f = (x/r_0)Pe_x^{-1/2}$ and $\xi_n = (x/r_0)Ra_x^{-1/2}$ which measure the curvature effect from each limit of mixed convection. For the entire mixed-convection regime, a single variable $\chi = [1 + (Ra_x/Pe_x)^{1/2}]^{-1}$ describes the mixed-convection effect, with the curvature parameter given by $\xi = (x/r_0)(Pe_x^{1/2} + Ra_x^{1/2})^{-1}$. In order to achieve better numerical accuracy, a finite difference technique is used to solve each of the systems of nonsimilar equations in the present study. Results are presented for the buoyancy assisting flow condition.

Analysis

Consider mixed convection from an impermeable vertical cylinder embedded in a porous medium. The surface of the cylinder is maintained at a uniform wall temperature T_w (UWT). In the analysis to follow, three approaches to mixed convection will be examined: 1) the effect of buoyancy on forced convection, 2) the effect of forced flow on free convection, and 3) the entire regime of mixed convection. The x coordinate is measured along the cylinder from the leading edge and the r coordinate is measured from the centerline of the cylinder. The gravitational acceleration g is acting downward along the cylinder, opposite to the x direction. Assuming low velocity and porosity, the Darcy model is employed in the analysis. Further assumptions include constant fluid properties and isotropic porous medium with uniform porosity. Also, the radius of the cylinder is taken to be much larger than the pore size of the medium so that the flow channeling effect near the cylinder can be neglected. In the present study, the non-Darcian and thermal dispersion effects are not considered.

The analysis will be carried out for upward forced flow with $T_w > T_\infty$ and downward forced flow $T_w < T_\infty$; i.e., for the buoyancy assisting flow condition. Under the Boussinesq and the boundary-layer approximations, the governing equations for the problem under consideration can be written as[2]

$$\frac{\partial}{\partial x}(ru) + \frac{\partial}{\partial r}(rv) = 0 \tag{1}$$

$$\frac{\partial}{\partial r}\left(\frac{1}{r}\frac{\partial \psi}{\partial r}\right) = \frac{K}{\mu}\rho g\beta \frac{\partial T}{\partial r} \tag{2}$$

$$\frac{\partial \psi}{\partial r}\frac{\partial T}{\partial x} - \frac{\partial \psi}{\partial x}\frac{\partial T}{\partial r} = \alpha \frac{\partial}{\partial r}\left(r\frac{\partial T}{\partial r}\right) \tag{3}$$

where ψ satisfies the continuity equation with $ru = \partial\psi/\partial r$ and $rv = -\partial\psi/\partial x$, with u and v denoting the Darcian velocity components in the x and r directions; ρ, μ, and β are the density, dynamic viscosity, and thermal expansion coefficient of the fluid, and K and α are the permeability and equivalent thermal diffusivity of the porous medium. The corresponding boundary conditions are

$$v = 0, \quad T = T_w \quad \text{at} \quad r = r_0$$
$$u \to u_\infty, \quad T \to T_\infty \quad \text{as} \quad r \to \infty \tag{4}$$

Next, the system of Eqs. (2) and (3) will be cast into a dimensionless form, separately for different regimes of mixed convection.

Effect of Buoyancy on Forced Convection

To transform Eqs. (2) and (3) from the (x, y) coordinates to the dimensionless coordinates $[\xi_f(x), \eta_f(x, y)]$ for the forced-convection-dominated regime, one introduces the following variables:

$$\eta_f = \frac{r^2 - r_0^2}{2r_0 x} Pe_x^{1/2}, \qquad \xi_f = \xi_f(x) \tag{5}$$

$$\psi = \alpha r_0 Pe_x^{1/2} f(\xi_f, \eta_f), \qquad \theta(\xi_f, \eta_f) = \frac{T - T_\infty}{T_w - T_\infty} \tag{6}$$

By substituting Eqs. (5) and (6) into Eqs. (2) and (3), the following system of equations is obtained:

$$f'' = \Omega\theta' \tag{7}$$

$$(1 + 2\xi_f\eta_f)\theta'' + \left(2\xi_f + \frac{1}{2}f\right)\theta' = \frac{1}{2}\xi_f\left(f'\frac{\partial\theta}{\partial\xi_f} - \theta'\frac{\partial f}{\partial\xi_f}\right) \tag{8}$$

The boundary conditions are

$$f(\xi_f, 0) + \xi_f\frac{\partial f}{\partial \xi_f}(\xi_f, 0) = 0 \quad \text{or} \quad f(\xi_f, 0) = 0$$
$$\theta(\xi_f, 0) = 1, \quad f'(\xi_f, \infty) = 1, \quad \theta(\xi_f, \infty) = 0 \tag{9}$$

In Eqs. (7–9) ξ_f has the expression

$$\xi_f = (x/r_0)Pe_x^{-1/2} \tag{10}$$

and Ω is given by

$$\Omega = Ra_x/Pe_x = \text{const for UWT} \tag{11}$$

with $Pe_x = u_\infty x/a$ and $Ra_x = g\beta|T_w - T_\infty|Kx/\nu\alpha$.

In the system of equations above, the primes denote partial differentiation with respect to η_f. Also, the variable ξ_f represents the curvature effect, while Ω represents the effect of buoyancy on forced convection. The case of $\Omega = 0$ represents pure forced convection and $\Omega = \infty$ represents pure free convection.

Note that for a flat plate, ξ_f goes to 0 ($r_0 \to \infty$) and the resulting equations become similar, which corresponds to the case studied by Hsieh et al.[7] under UWT. Physical quantities of interest include the velocity components u and v in the x and r directions, the local wall shear stress τ_w defined as $\tau_w = \mu(\partial u/\partial r)_{r=r_0}$, and the local Nusselt number $Nu = hx/k$, where $h = q_w/(T_w - T_\infty)$. They can be expressed by

$$u = u_\infty f'(\xi_f, \eta_f) \tag{12}$$

$$v = -\frac{1}{2}\frac{\alpha}{x}(1 + 2\xi_f\eta_f)^{-1/2}Pe_x^{1/2}\left(f + \xi_f\frac{\partial f}{\partial\xi_f} - \eta_f f'\right) \tag{13}$$

$$\tau_w = \mu\frac{u_\infty}{x}Pe_x^{1/2}f''(\xi_f, 0) \tag{14}$$

$$Nu_x = -Pe_x^{1/2}\theta'(\xi_f, 0) \tag{15}$$

By finding $\bar{h}$ over L, one can find $\overline{Nu}$ as

$$\overline{Nu} = 2Pe_L^{1/2}\xi_{f_L}^{-1}\int_0^{\xi_{f_L}}[-\theta'(\xi_f, 0)]\,d\xi_f \tag{16}$$

In Eq. (16) Pe_L and ξ_{f_L} are the values of Pe_x and ξ_x evaluated at $x = L$.

Effect of Forced Flow on Free Convection

In this free-convection-dominated regime, a different set of dimensionless variables are introduced to examine the effect of forced flow on free convection. They are

$$\eta_n = \frac{r^2 - r_0^2}{2r_0x} Ra_x^{1/2}, \qquad \xi_n = \xi_n(x) \tag{17}$$

$$\psi = \alpha r_0 Ra_x^{1/2} f(\xi_n, \eta_n), \qquad \theta(\xi_n, \eta_n) = \frac{T - T_\infty}{T_w - T_\infty} \tag{18}$$

By substituting Eqs. (17) and (18) into the governing Eqs. (2) and (3), one arrives at

$$f'' = \theta' \tag{19}$$

$$(1 + 2\xi_n\eta_n)\theta'' + \left(2\xi_n + \frac{1}{2}f\right)\theta' = \frac{1}{2}\xi_n\left(f'\frac{\partial\theta}{\partial\xi_n} - \theta'\frac{\partial f}{\partial\xi_n}\right) \tag{20}$$

with the boundary conditions

$$\begin{aligned} &f(\xi_n, 0) + \xi_n\frac{\partial f}{\partial\xi_n}(\xi_n, 0) = 0 \quad \text{or} \quad f(\xi_n, 0) = 0 \\ &\theta(\xi_n, 0) = 1, \quad f'(\xi_n, \infty) = \Omega^{-1}, \quad \theta(\xi_n, \infty) = 0 \end{aligned} \tag{21}$$

In Eqs. (19–21) the nonsimilarity parameter ξ_n has the expression

$$\xi_n = (x/r_0)Ra_x^{-1/2} \tag{22}$$

and the primes denote partial differentiation with respect to η_n. Again, the ξ_n variable measures the effect of curvature. It is noted here that ξ_n is related to ξ_f by $\xi_n = \xi_f\Omega^{-1/2}$.

The velocity components u and v, the local wall shear stress, and the local Nusselt number for this case are found to be

$$u = (\alpha/x)Ra_x f'(\xi_n, \eta) \tag{23}$$

$$v = -\frac{1}{2}\frac{\alpha}{x}(1 + 2\xi_n\eta_n)^{-1/2}Ra_x^{1/2}\left(f + \xi_n\frac{\partial f}{\partial\xi_n} - \eta_n f'\right) \tag{24}$$

$$\tau_w = \frac{\mu\alpha}{x^2}Ra_x^{3/2}f''(\xi_n, 0) \tag{25}$$

$$Nu_x = -Ra_x^{1/2}\theta'(\xi_n, 0) \tag{26}$$

One can also find $\overline{Nu}$ as

$$\overline{Nu} = 2Ra_L^{1/2}\xi_{n_L}^{-1}\int_0^{\xi_{n_L}}[-\theta'(\xi_n, 0)]\,d\xi_n \tag{27}$$

In Eq. (27) Ra_L and ξ_{n_L} are the values of Ra_x and ξ_n evaluated at $x = L$.

It is observed that solutions of the two systems of Eqs. (7–9) and (19–21), could cover the entire mixed-convection regime from the pure forced-convection limit to the pure free-convection limit. Unfortunately, when Ω becomes too large or when the forced flow parameter Ω^{-1} becomes too large, numerical difficulties develop in the solution of Eqs. (7–9) or Eqs. (19–21). This situation can be avoided with a universal analysis for the entire mixed-convection regime, which is presented below.

Entire Regime of Mixed Convection

In order to obtain a system of equations applicable to the entire regime of mixed convection, one introduces the following dimensionless variables:

$$\eta = \frac{r^2 - r_0^2}{2r_0x}Pe_x^{1/2}\chi^{-1} = \frac{r^2 - r_0^2}{2r_0x}(Pe_x^{1/2} + Ra_x^{1/2}), \quad \xi = \xi(x) \tag{28}$$

$$\psi = \alpha r_0 Pe_x^{1/2}\chi^{-1}f(\xi, \eta) = \alpha r_0(Pe_x^{1/2} + Ra_x^{1/2})f(\xi, \eta)$$

$$\theta(\xi, \eta) = \frac{T - T_\infty}{T_w - T_\infty} \tag{29}$$

where

$$\chi = \frac{1}{1 + (Ra_x/Pe_x)^{1/2}} = \text{const for UWT} \tag{30}$$

Substituting Eqs. (28) and (29) into Eqs. (2) and (3) gives

$$f'' - (1 - \chi)^2\theta' = 0 \tag{31}$$

$$(1 + 2\xi\eta)\theta'' + \left(2\xi + \frac{1}{2}f\right)\theta' = \frac{1}{2}\xi\left(f'\frac{\partial\theta}{\partial\xi} - \theta'\frac{\partial f}{\partial\xi}\right) \tag{32}$$

The corresponding boundary conditions are

$$\begin{aligned} &f(\xi, 0) + \xi\frac{\partial f}{\partial\xi}(\xi, 0) = 0 \quad \text{or} \quad f(\xi, 0) = 0 \\ &\theta(\xi, 0) = 1, \quad f'(\xi, \infty) = \chi^2, \quad \theta(\xi, \infty) = 0 \end{aligned} \tag{33}$$

where ξ is now given by

$$\xi = (x/r_0)(Pe_x^{1/2} + Ra_x^{1/2})^{-1} \tag{34}$$

The parameter χ is the mixed-convection parameter. A value of $\chi = 0$ corresponds to pure free convection, while $\chi = 1$ represents pure forced convection. The entire regime of mixed convection corresponds to values of χ between 0 and 1.

The velocity components u and v, the local wall shear stress, and the local Nusselt number for this case have the expressions

$$u = (\alpha/x)(Pe_x^{1/2} + Ra_x^{1/2})^2 f'(\xi, \eta) \tag{35}$$

$$v = -\frac{1}{2}\frac{\alpha}{x}(Pe_x^{1/2} + Ra_x^{1/2})(1 + 2\xi\eta)^{-1/2}\left(f + \xi\frac{\partial f}{\partial\xi} - \eta f'\right) \tag{36}$$

$$\begin{aligned} \tau_w &= (\mu\alpha/x^2)\chi^{-3}Pe_x^{3/2}f''(\xi, 0) \\ &= (\mu\alpha/x^2)(Pe_x^{1/2} + Ra_x^{1/2})^3 f''(\xi, 0) \end{aligned} \tag{37}$$

$$Nu_x = -Pe_x^{1/2}\chi^{-1}\theta'(\xi, 0) = -(Pe_x^{1/2} + Ra_x^{1/2})\theta'(\xi, 0) \tag{38}$$

The average Nusselt number can be expressed, with $\chi_L = \chi$ = const for UWT, as

$$\begin{aligned} \overline{Nu} &= 2Pe_L^{1/2}\chi_L^{-1}\xi_L^{-1}\int_0^{\xi_L}[-\theta'(\xi, 0)]\,d\xi \\ &= 2(Pe_L^{1/2} + Ra_L^{1/2})\xi_L^{-1}\int_0^{\xi_L}[-\theta'(\xi, 0)]\,d\xi \end{aligned} \tag{39}$$

Results and Discussion

The systems of equations, Eqs. (7–9), (19–21), and (31–33), were solved using the Runge-Kutta integration method

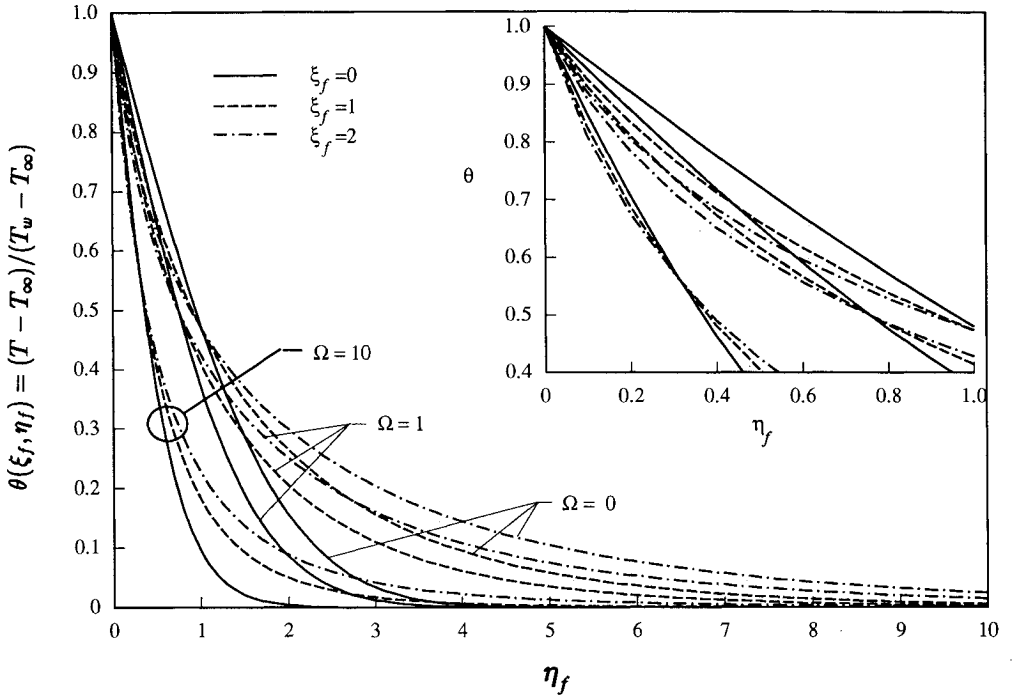

Fig. 1 Dimensionless temperature profiles at selected values of ξ_f and Ω.

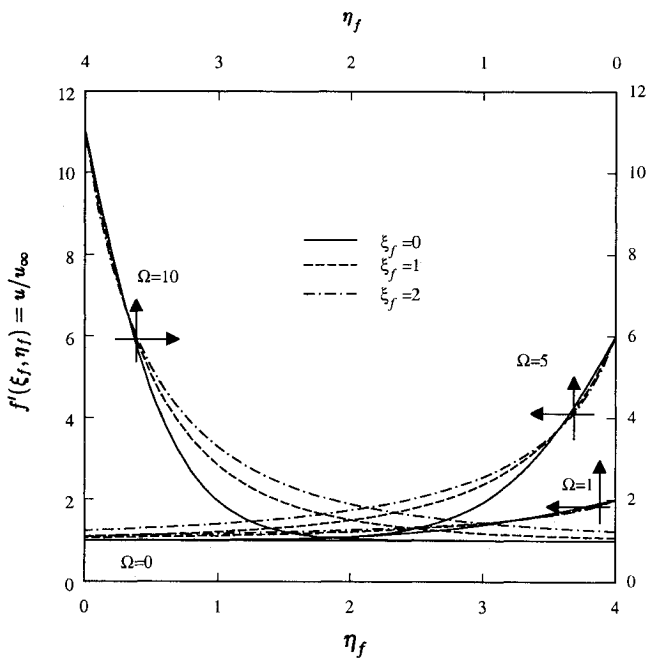

Fig. 2 Dimensionless velocity profiles at selected values of ξ_f and Ω.

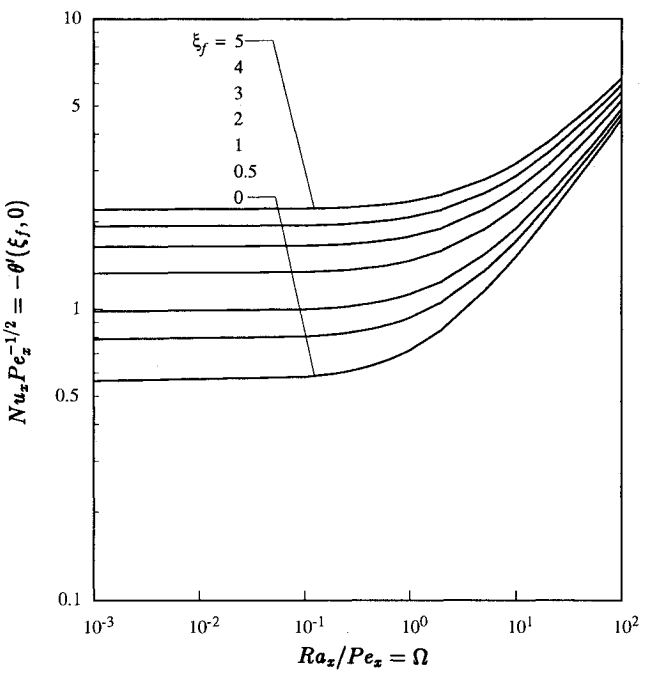

Fig. 3 Local Nusselt number variation at selected values of ξ_f.

along with a shooting method at $\xi_f = \xi_n = \xi = 0$. The numerical solutions for ξ_f, ξ_n, $\xi > 0$ were then carried out using a finite difference method similar to that of Cebeci and Bradshaw.[15] The details of the solution method are omitted here to conserve space. It is worth noting that step sizes of $\Delta\eta = 0.02$ and $\Delta\xi = 0.1$ were found to be satisfactory for a convergence criterion of 10^{-4} in nearly all cases. The starting values of η_∞ ranged from 8 for pure forced convection to 16 for pure free convection.

Numerical results of interest for the buoyancy assisting condition are presented in this section. They are good for upward forced flow with $T_w > T_\infty$ and downward forced flow with $T_w < T_\infty$. Solutions were found for $0 \le \xi_f, \xi_n, \xi \le 5$. For typical values of $Ra_L = 10^3$ and $Pe_L = 10^3$, the range of L/r_0 values is $158.1 \le L/r_0 \le 316.2$. For a radius as small as 5 cm, this corresponds to L of 7.9–15.8 m.

Results for the temperature and velocity profiles, $\theta(\xi_f, \eta_f)$ and $f'(\xi_f, \eta_f)$, are shown in Figs. 1 and 2 for different values of ξ_f and Ω. Figure 1 shows that the thermal boundary-layer thickness increases with increasing curvature and decreases with increasing buoyancy. It is also noted that higher values of curvature and buoyancy give rise to larger temperature gradients at the surface. Figure 2 shows an increase in the slip velocity and momentum boundary-layer thickness as curvature and buoyancy force increase. Figures 3 and 4 show the variation of the local Nusselt number as mixed convection is approached from the pure forced-convection limit ($\Omega = Ra_x/Pe_x = 0$) and pure free-convection limit ($\Omega^{-1} = Pe_x/Ra_x = 0$), respectively. It is noted from these two figures that increases in curvature and buoyancy effect (Ra_x/Pe_x) or forced flow effect (Pe_x/Ra_x) produce an increase in the local Nusselt

Table 1 Values of $-\theta'(\xi, 0)$ at selected values of ξ_f and Ω, and ξ_n and Ω^{-1}

	$-\theta'(\xi_f, 0)$			
$\Omega = Ra_x/Pe_x$	$\xi_f = 0$	$\xi_f = 1$	$\xi_f = 2$	$\xi_f = 5$
0.0	0.5642	0.9839	1.3286	2.2044
0.1	0.5819	0.9992	1.3436	2.2201
0.2	0.6000	1.0142	1.3584	2.2354
0.3	0.6156	1.0289	1.3728	2.2505
0.4	0.6317	1.0433	1.3870	2.2653
0.5	0.6474	1.0574	1.4009	2.2799
0.6	0.6627	1.0712	1.4146	2.2941
0.7	0.6777	1.0848	1.4280	2.3084
0.8	0.6923	1.0981	1.4412	2.3225
0.9	0.7066	1.1113	1.4542	2.3362
1.0	0.7206	1.1241	1.4670	2.3490
	$-\theta'(\xi_n, 0)$			
$\Omega^{-1} = Pe_x/Ra_x$	$\xi_n = 0$	$\xi_n = 1$	$\xi_n = 2$	$\xi_n = 5$
0.0	0.4438	0.7778	1.0623	1.7998
0.1	0.4795	0.8313	1.1218	1.8957
0.2	0.5123	0.8724	1.1797	1.9732
0.3	0.5430	0.9140	1.2221	2.0196
0.4	0.5719	0.9495	1.2645	2.0744
0.5	0.5993	0.9838	1.3119	2.1625
0.6	0.6255	1.0143	1.3403	2.1757
0.7	0.6506	1.0428	1.3735	2.2200
0.8	0.6748	1.0727	1.4118	2.2883
0.9	0.6981	1.0981	1.4365	2.3043
1.0	0.7206	1.1246	1.4617	2.3605

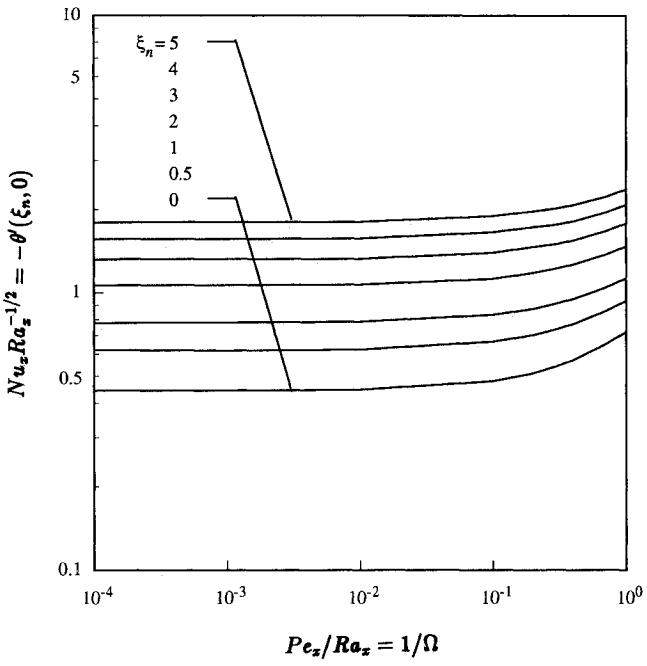

Fig. 4 Local Nusselt number variation at selected values of ξ_n.

number. In Fig. 3 it is seen that all curves will converge to one point in the free-convection limit. Table 1 shows the $-\theta'(\xi_f, 0)$ and $-\theta'(\xi_n, 0)$ values for selected values of ξ_f and Ω, and ξ_n and Ω^{-1}. The corresponding $f''(\xi_f, 0)$ and $f''(\xi_n, 0)$ values can be obtained from Eqs. (7) and (19) evaluated at $\eta_f = \eta_n = 0$, along with the $-\theta'(\xi_f, 0)$ and $-\theta'(\xi_n, 0)$ values given in the table. These values are needed for calculating the local Nusselt number and the local wall shear stress.

A Nusselt number correlation equation for the case of pure forced convection can be found using the technique of least squares. It is given by

$$Nu_f = f_1(\xi_f) Pe_x^{1/2} \tag{40}$$

where

$$f_1(\xi_f) = 0.5650 + 0.4424\xi_f - 0.0377\xi_f^2 + 0.0029\xi_f^3 \tag{41}$$

For the case of pure free convection, the correlation equation for the local Nusselt number is

$$Nu_n = f_2(\xi_n) Ra_x^{1/2} \tag{42}$$

where

$$f_2(\xi_n) = 0.4457 + 0.3509\xi_n - 0.2482\xi_n^2 + 0.0019\xi_n^3 \tag{43}$$

These local Nusselt number correlation equations fit the numerical results within 5%.

Next, by using a modified version of Churchill's method,[16] an equation for the local Nusselt number in mixed convection Nu_x can be expressed as

$$(Nu_x/Nu_f)^m = 1 + (Nu_n/Nu_f)^m \tag{44}$$

In the case studied here, Eq. (44) can be expressed as

$$\frac{Nu_x Pe_x^{-1/2}}{f_1(\xi_f)} = \left\{1 + \left[\frac{f_2(\xi_f \Omega^{-1/2})}{f_1(\xi_f)}\,\Omega^{1/2}\right]^{m_1(\xi_f)}\right\}^{1/m_1(\xi_f)} \tag{45}$$

where

$$m_1(\xi_f) = 2 + 0.7221\xi_f \tag{46}$$

The corresponding average Nusselt numbers for the cases above can be expressed as

$$\overline{Nu_f} = 2F_1(\xi_{f_L}) Pe_L^{1/2} \tag{47}$$

$$\overline{Nu_n} = 2F_2(\xi_{n_L}) Ra_L^{1/2} \tag{48}$$

$$\frac{\overline{Nu} Pe_L^{-1/2}}{2F_1(\xi_{f_L})} = \left\{1 + \left[\frac{F_2(\xi_{f_L}\Omega^{-1/2})}{F_1(\xi_{f_L})}\,\Omega^{1/2}\right]^{m_1(\xi_{fL})}\right\}^{1/m_1(\xi_{fL})} \tag{49}$$

where

$$F_1(\xi_{f_L}) = 0.5650 + 0.2212\xi_{f_L} - 0.0126\xi_{f_L}^2 + 0.00073\xi_{f_L}^3 \tag{50}$$

$$F_2(\xi_{f_L}) = 0.4457 + 0.1754\xi_{n_L} - 0.0827\xi_{n_L}^2 + 0.00048\xi_{n_L}^3 \tag{51}$$

The above correlation equations for the local and average Nusselt numbers provide results that agree fairly well with the numerically predicted values. The maximum deviation between the two is about 10%.

Figures 5 and 6 show temperature and velocity profiles for the entire regime of mixed convection. From Fig. 5 it is seen that an increase in the curvature at a given value of χ increases the thermal boundary-layer thickness. Also, increasing the value of χ at a given value of ξ decreases the thermal boundary-layer thickness. However, for a given ξ, the wall temperature gradient reaches a minimum value at some intermediate value of χ and has a maximum when $\chi = 1$. Figure 6 shows an increase in momentum boundary-layer thickness as χ decreases from 1 to 0.

The variation of the local Nusselt number for the entire regime is shown in Fig. 7. It is observed that all curves in Fig. 7 reach a local minimum at a value between $0 < \chi < 1$. However, as noted by Hsieh et al.,[6] this minimum does not imply a corresponding minimum value in the local Nusselt number. If one considers an intermediate point at $\chi = 0.5$, with $\xi = 2$ and $Ra_x = Pe_x = 10^3$, the local Nusselt number

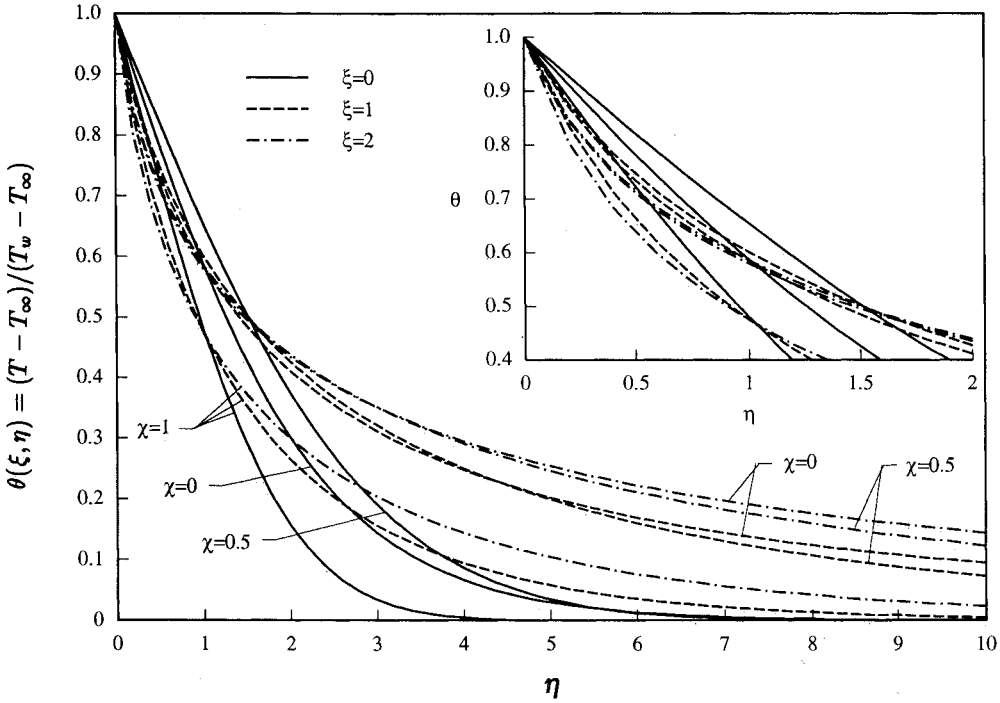

Fig. 5 Dimensionless temperature profiles at selected values of ξ and χ.

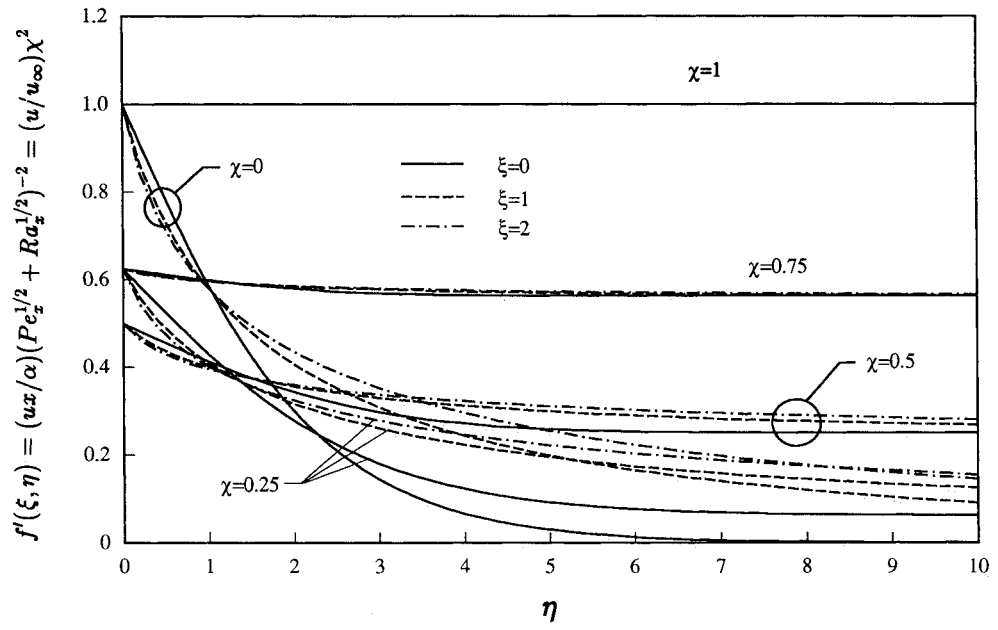

Fig. 6 Dimensionless velocity profiles at selected values of ξ and χ.

for mixed convection has a value $Nu_x = 65.69$, whereas the local Nusselt numbers for pure forced convection ($\chi = 1$) and pure free convection ($\chi = 0$) are $Nu_x = 42.04$ and $Nu_x = 33.56$, respectively. The values of $-\theta'(\xi, 0)$ for $0 \le \xi \le 5$ and $0 \le \chi \le 1$ are listed in Table 2. The corresponding $f''(\xi, 0)$ value can be found from Eq. (31), evaluated at $\eta = 0$, along with the $-\theta'(\xi, 0)$ values.

The mixed-convection local Nusselt number for the entire regime can be expressed by the correlation

$$\frac{Nu_x(Pe_x^{1/2} + Ra_x^{1/2})^{-1}}{f_1(\xi)} = \left\{\chi^{m_2(\xi)} + \left[(1 - \chi)\frac{f_2(\xi)}{f_1(\xi)}\right]^{m_2(\xi)}\right\}^{1/m_2(\xi)} \quad (52)$$

where

$$m_2(\xi) = 2 - 0.1199\xi \quad (53)$$

and f_1 and f_2 are as given by Eqs. (42) and (43). The corresponding average Nusselt can be correlated as

$$\frac{\overline{Nu}(Pe_L^{1/2} + Ra_L^{1/2})^{-1}}{2F_1(\xi_L)} = \left\{\chi^{m_2(\xi_L)} + \left[(1 - \chi)\frac{F_2(\xi_L)}{F_1(\xi_L)}\right]^{m_2(\xi_L)}\right\}^{1/m_2(\xi_L)} \quad (54)$$

where F_1 and F_2 are as given by Eqs. (50) and (51). The above correlation equations fit the numerical data to within 10%.

To give the range of Ω and χ values corresponding to mixed convection, a 5% departure rule was applied to the correlation Eqs. (45) and (52) for the local Nusselt number in mixed convection. These ranges for forced convection, mixed convection, and free convection are presented in Table 3.

A comparison of the present results with experimental data would be appropriate. However, to the best knowledge of the authors, no such data seem to be available for mixed convection along a vertical cylinder in a porous medium. The only comparison that can be made is with the experimental results of Cheng et al.[17] for natural convection ($\chi = 0$) along a vertical plate ($\xi = 0$). A good agreement is found to exist between the predicted and measured results for this limiting case.

As a final note, inclusion of the non-Darcian effects involving flow inertia and viscous shear force with no-slip boundary has been found to decrease the surface heat transfer rate.[18-20] On the other hand, the thermal dispersion effect has been found to increase the rate of heat transfer.[19,20] These effects were not considered in the present study. It should be noted that Ref. 19 appeared in the literature after the review process of this article was completed. That work, however, is limited to forced-convection-dominated regime.

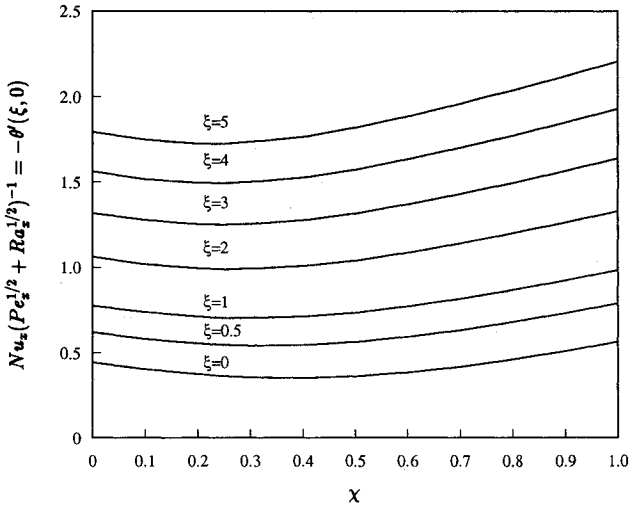

Fig. 7 Local Nusselt number variation at selected values of ξ.

Table 2 Values of $-\theta'(\xi, 0)$ at selected values of ξ and χ

	$-\theta'(\xi, 0)$			
χ	$\xi = 0$	$\xi = 1$	$\xi = 2$	$\xi = 5$
0.0	0.4438	0.7749	1.0613	1.7941
0.1	0.4035	0.7386	1.0162	1.7494
0.2	0.3732	0.7113	0.9928	1.7250
0.3	0.3550	0.7032	0.9909	1.7360
0.4	0.3506	0.7111	1.0061	1.7664
0.5	0.3603	0.7347	1.0388	1.8193
0.6	0.3832	0.7708	1.0846	1.8857
0.7	0.4173	0.8159	1.1387	1.9599
0.8	0.4602	0.8679	1.1987	2.0402
0.9	0.5098	0.9243	1.2626	2.1232
1.0	0.5642	0.9841	1.3293	2.2078

Concluding Remarks

The problem of mixed convection along an isothermal vertical cylinder in a porous medium has been examined based on the Darcy model and without the thermal dispersion effect. The nonsimilar variables ξ_f, ξ_n, and ξ have been introduced to show the effect of curvature, while the parameters Ω, Ω^{-1}, and χ govern the extents of buoyancy, freestream velocity, and the combined effect on the thermal and flowfields. Temperature and velocity profiles, local Nusselt number, and correlation equations for the local and average Nusselt numbers are presented. The regimes of forced, mixed, and free convection are also established.

Acknowledgment

The present study was supported in part by a Grant from the University of Missouri System (Weldon Spring/Chen/91-92).

References

[1]Cheng, P., and Minkowycz, W. J., "Free Convection About a Vertical Flat Plate Embedded in a Porous Medium with Application to Heat Transfer from a Dike," *Journal of Geophysical Research*, Vol. 82, No. 14, 1977, pp. 2040-2044.

[2]Minkowycz, W. J., and Cheng, P., "Free Convection About a Vertical Cylinder Embedded in a Porous Medium," *International Journal of Heat and Mass Transfer*, Vol. 19, No. 7, 1976, pp. 805-813.

[3]Ranganathan, P., and Viskanta, R., "Mixed Convection Boundary-Layer Flow Along a Vertical Surface in a Porous Medium," *Numerical Heat Transfer*, Vol. 7, No. 3, 1984, pp. 305-317.

[4]Hsu, C. T., and Cheng, P., "The Brinkman Model for Natural Convection About a Semi-Infinite Vertical Flat Plate in a Porous Medium," *International Journal of Heat and Mass Transfer*, Vol. 28, No. 3, 1985, pp. 683-697.

[5]Hong, J. T., Yamada, Y., and Tien, C. L., "Effects of Non-Darcian and Nonuniform Porosity on Vertical-Plate Natural Convection in Porous Media," *Journal of Heat Transfer*, Vol. 109, May 1987, pp. 356-362.

[6]Lai, F. C., and Kulacki, F. A., "Non-Darcy Mixed Convection Along a Vertical Wall in a Saturated Porous Medium," *Journal of Heat Transfer*, Vol. 113, Feb. 1991, pp. 252-255.

[7]Hsieh, J. C., Chen, T. S., and Armaly, B. F., "Nonsimilarity Solutions for Mixed Convection from Vertical Surfaces in Porous Media: Variable Surface Temperature or Heat Flux," *International Journal of Heat and Mass Transfer* (to be published).

[8]Aldoss, T. K., Chen, T. S., and Armaly, B. F., "Nonsimilarity Solutions for Mixed Convection from Horizontal Surfaces in a Porous Medium—Variable Wall Temperature," *International Journal of Heat and Mass Transfer*, Vol. 36, No. 2, 1993, pp. 471-477.

[9]Aldoss, T. K., Chen, T. S., and Armaly, B. F., "Nonsimilarity Solutions for Mixed Convection from Horizontal Surfaces in a Porous Medium—Variable Surface Heat Flux," *International Journal of Heat and Mass Transfer*, Vol. 36, No. 2, 1993, pp. 463-470.

[10]Hsieh, J. C., Chen, T. S., and Armaly, B. F., "Mixed Convection Along a Non-Isothermal Vertical Flat Plate Embedded in a Porous Medium," *International Journal of Heat and Mass Transfer* (to be published).

[11]Aldoss, T. K., Chen, T. S., and Armaly, B. F., "Mixed Convection over Non-Isothermal Horizontal Surfaces in a Porous Medium," *Numerical Heat Transfer* (submitted for publication).

[12]Minkowycz, W. J., Cheng, P., and Chang, C. H., "Mixed Convection About a Nonisothermal Cylinder and Sphere in a Porous Medium," *Numerical Heat Transfer*, Vol. 8, No. 3, 1985, pp. 349-359.

[13]Hsu, C. T., and Cheng, P., "Thermal Dispersion in a Porous

Table 3 Range of Ω and χ values for forced, mixed, and free convection

Curvature	Forced convection		Mixed convection		Free convection	
ξ_f or ξ	Ω	χ	Ω	χ	Ω	χ
0	0-0.15	1-0.82	0.15-19.63	0.82-0.11	19.63-∞	0.11-0
1	0-0.24	1-0.80	0.24-157.11	0.80-0.11	157.11-∞	0.11-0
2	0-0.34	1-0.84	0.34-288.05	0.84-0.09	288.05-∞	0.09-0
5	0-0.95	1-0.93	0.95-501.29	0.93-0.02	501.29-∞	0.02-0

Medium," *International Journal of Heat and Mass Transfer*, Vol. 33, No. 8, 1990, pp. 1587–1597.

[14]Kaviany, M., *Principles of Heat Transfer in Porous Media*, Springer-Verlag, New York, 1991.

[15]Cebeci, T., and Bradshaw, P., *Momentum Transfer in Boundary Layers*, Hemisphere, Washington, DC, 1977, Chaps. 7 and 8.

[16]Churchill, S. W., "A Comprehensive Correlating Equation for Laminar Assisting, Forced and Free Convection," *AIChE Journal*, Vol. 23, No. 1, 1977, pp. 10–16.

[17]Cheng, P., Ali, C. L., and Verma, A. K., "An Experimental Study of Non-Darcian Effects in Free Convection in a Saturated Porous Medium," *Letters in Heat and Mass Transfer*, Vol. 8, No. 4, 1981, pp. 261–265.

[18]Vafai, K., and Tien, C. L., "Boundary and Inertia Effects on Flow and Heat Transfer in Porous Media," *International Journal of Heat and Mass Transfer*, Vol. 24, No. 2, 1981, pp. 195–203.

[19]Chen, C. H., and Chen, C. K., "Non-Dimensional Mixed Convection Along a Vertical Plate in a Porous Medium," *Applied Mathematical Modelling*, Vol. 14, Sept. 1990, pp. 482–488.

[20]Chen, C. K., Chen, C. H., Minkowycz, W. J., and Gill, U. S., "Non-Darcian Effects on Mixed Convection About a Vertical Cylinder Embedded in a Saturated Porous Medium," *International Journal of Heat and Mass Transfer*, Vol. 35, No. 11, 1992, pp. 3041–3046.